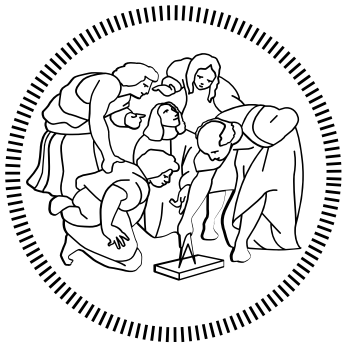

POLITECNICO
MILANO 1863

Modeling of a blow-down propulsion system

Course of Space Propulsion
Academic Year 2023-2024

Lockheed Martini Group

Alessandro Pallotta	alessandro1.pallotta@mail.polimi.it	10712370
Alex Cristian Turcu	alexcristian.turcu@mail.polimi.it	10711624
Chiara Poli	chiara3.poli@mail.polimi.it	10731504
Daniele Paternoster	daniele.paternoster@mail.polimi.it	10836125
Paolo Vanelli	paolo.vanelli@mail.polimi.it	10730510
Riccardo Vidari	riccardo.vidari@mail.polimi.it	10711828

Contents

Nomenclature

Acronyms

LRE	Liquid Rocket Engine
LOX	Liquid Oxygen
RP-1	RP-1 fuel
AM	Additive Manufacturing

Symbols

a	[m/s]	Speed of sound
A	[m^2]	Area
B	[-]	Blow-down ratio
c_P	[J/kg K]	Specific heat at constant pressure
c_T	[-]	Thrust coefficient
c^*	[m/s]	Characteristic velocity
C_d	[-]	Discharge coefficient
D	[m]	Diameter
E	[m/s]	Erosion rate
f	[-]	Darcy friction factor
h	[W/m^2 K]	Convective heat transfer coefficient
H	[m]	Height
i	[-]	First iteration index
I_{sp}	[s]	Specific impulse
I_{tot}	[N s]	Total impulse
j	[-]	Second iteration index
k	[m^{-1}]	Curvature
K	[-]	Pressure loss coefficient
L	[m]	Length
L^*	[m]	Characteristic length
m	[kg]	Mass
$\dot{m}$	[m/s]	Mass flow rate
M	[-]	Mach number
$\mathbb{M}$	[kg/mol]	Molar mass
N	[-]	Number of
O/F	[-]	Oxidizer to fuel ratio
$\overline{O/F}$	[-]	Mean O/F ratio
p	[Pa]	Pressure
Δp	[Pa]	Pressure loss / difference
Pr	[-]	Prandtl number
$\dot{q}$	[W/m^2]	Heat flux
$\dot{Q}$	[W]	Heat transfer rate
r	[-]	Recovery factor
R	[J/kg K]	Specific gas constant
$\mathcal{R}$	[J/mol K]	Universal gas constant
Re	[-]	Reynolds number
Re'	[-]	Modified Reynolds number
t	[s]	Time
Δt	[s]	Time step
T	[K]	Temperature
$\mathbb{T}$	[N]	Thrust
u	[m/s]	Velocity
V	[m^3]	Volume
ΔV	[m^3]	Volume change
α_{AM}	[deg]	Deposition angle of AM
α_{con}	[deg]	Convergent semi-aperture angle
β	[%]	Injector pressure drop as percentage of initial combustion chamber pressure
γ	[-]	Heat capacity ratio
ε	[-]	Area ratio
λ	[-]	Nozzle losses coefficient
μ	[Pa s]	Dynamic viscosity
ρ	[kg/m^3]	Density
σ	[-]	Correction factor across boundary layer

Subscripts

aw	Adiabatic wall
c	Combustion chamber
cea	From CEAM software
con	Convergent
e	Nozzle exit
eff	Effective
f	Final
fd	Feeding lines
fu	Fuel
i	Initial
id	Ideal
inj	Injector
max	Maximum
min	Minimum
ox	Oxidizer
p	Propellants
pr	Pressurizer gas
r	Real
t	Nozzle throat
tc	Thrust chamber
tk	Tank
tot	Total
wg	Gas side wall

1 Introduction and literature overview

In this work a preliminary design of a 1 kN semi-cryogenic LRE (LOX/RP-1) equipped with a blow-down feeding system is discussed. In particular, a first literature analysis was done in order to review previous studies regarding this particular architecture. Recent developments in additive manufacture (AM) techniques were analyzed to obtain some knowledge regarding processes and precision of this new frontier. Moreover, due the reduced size of this system, some criticalities regarding boundary layer and erosion losses were researched. The second part of the paper aim at designing the engine with some imposed initial conditions and some assumptions. The whole dimensioning of the system, including the tanks and feeding lines, is carried on including the dynamics of the system. The final sizing will accomplish the maximization of the total impulse, with the initial and final constraints. An off-design analysis is then performed to quantify the performances with nozzle losses and AM uncertainties. Finally, a feasibility analysis of nozzle fuel cooling is discussed.

1.1 Blow-down heritage

The blow-down architecture is the simplest feeding technique for LRE since it does not require additional pressurizing gas tanks with failure-prone pressure regulator valves nor complex turbomachinery. The scheme includes only two liquid propellant tanks filled with helium or nitrogen, eventually separated by a membrane. The major downsides of this simplicity is relative to the non-stationarity of the tank pressures that induce chamber pressure drop, decrease of propellant mass flow rate and as a consequence O/F ratio variation. This chain of events degrades performances overtime and must be carefully evaluated since combustion efficiency relies upon viable domains of injection pressure and correct mass flow ratio. The interest on blow-down is although justified with respect to well-known pressure regulated feed system since this last can also manifest some criticalities in terms of long-term reliability. In particular, propulsion systems play crucial roles for mission success, such as long interplanetary trips, and they must ensure failure-free lifetime. This is a major concern when focusing on pressure regulated feeding lines in which a pressure regulator valve is present. This kind of elements can be quite complex and hence add a weakness for the whole system[1]. Considering these facts, a blow-down type architecture could be of interest since it decrease system complexity. Moreover, different feasibility analysis for blow-down units are present in the literature in which also an external re-pressurization tank is considered[2]. This is an upgrade that allows to recover performance of the feeding pressure and hence combustion properties. Although the valve complexity is removed since a pyro valve can be used to discharge the gas with a single shot application, the eventual re-pressurization can be a crucial point as the sudden change in pressure could induce unwanted instabilities. Other configurations could foresee the use of a Venturi valve to maintain constant mass flow rate by cavitating the liquid and choking the flow on the feeding line. However, neither extra tank nor Venturi valves will be considered in this work in order to meet the requirements presented in subsection 2.1.
The whole evaluation of the dynamics of the examined propulsion system was not based upon previous works, instead a self-made model was developed.

1.2 Additive manufacturing state of art

1.3 Analysis of losses

2 Modelling of propulsion system: DRY-1

The workflow for the sizing of DRY-1 is introduced by Figure 1 and it is divided into three stages:

- **Input data**: the problem is set up.
- **Nominal sizing**: the system is sized according to initial conditions and general assumptions.
- **System dynamics**: an iterative process is set up to model the blow-down dynamics and finalize the sizing.

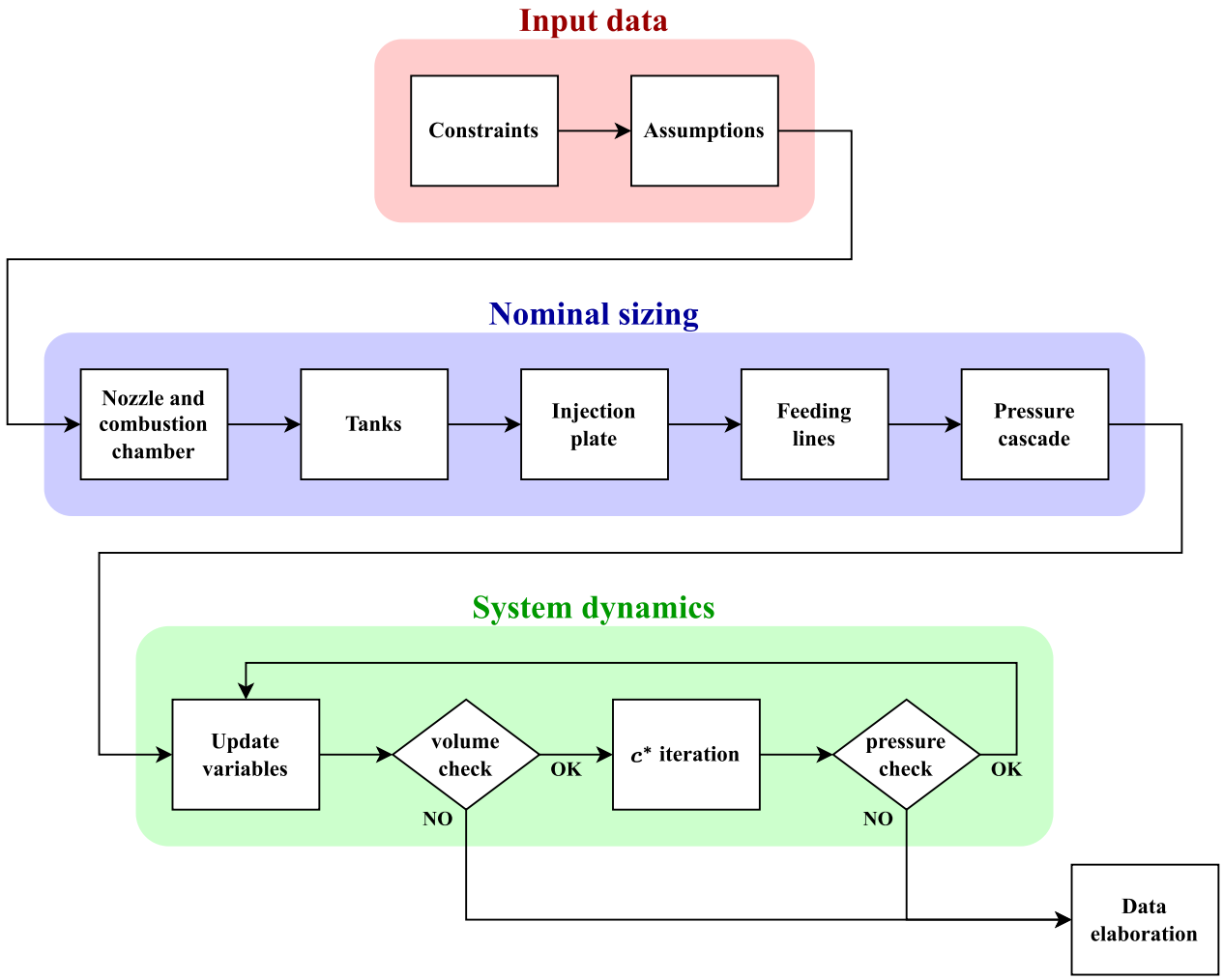

Figure 1: Flowchart of the simulation model

2.1 Input data

The input data defined different kind of requirements, related to operability environment, engine performance, size constraints, chemistry, architecture and manufacturing techniques. Regardless of the development of the engine design, the system shall respect the following pinpoints:

- **Environment**: vacuum for the whole operation.
- **Thrust** $\mathbb{T}$: initial magnitude of 1 kN, no lower boundary.
- **Chamber pressure** p_c: initial value of 50 bar, always above 20 bar throughout the whole mission.
- **Allocated space**: tanks, combustion chamber and convergent nozzle occupancy is exactly 80% of the volume occupied by a cylinder of 1 meter diameter and 2 meter length. No bounds on the extension of the divergent.
- **Propellants**: semi-cryogenic couple of LOX and RP-1.
- **Architecture**: blow-down type.
- **Manufacturing**: all the system is produced in AM, no restriction on material nor techniques.

The nominal sizing refers to the design of the overall system considering the imposed initial constraints as static conditions. This design choice was dictated by the dynamics of the blow-down system, which imposes the maximum flow rate at the beginning of the mission, leading to the oversizing of the engine throughout the rest of the mission.
Various hypothesis were necessary to develop the system, this values are reported in Table 1.

O/F [-]	ε [-]	ε_{con} [-]	L^* [m]
2.42	300	10	1.143

Table 1: Hypothesis from literature and previous design

The choices of L^* and O/F were only dictated by the propellant couple[3], while ε was chosen as the characteristic of the engine refers to an in-space application[4]. Regarding the value of ε_{con} a mean value between 5 and 15 was taken. Smaller values entails longer combustion chamber and small cross sectional area, with large pressure drops. Larger values refers to bigger chamber cross sectional area, with limited length for the combustion. From the literature the suggestion for the choice of this value is to refer to previous successful engines design, considering the same application[5]. Therefore, a 400 N bi-propellant apogee motor was taken as reference and revealed a value of $\varepsilon_{con} \approx 10$[4].

2.2 Nominal sizing

After defining the main input data, the workflow is carried out as shown in Figure 1. All the combustion simulations were performed with Nasa-CEA software, implemented in Matlab (CEAM). In particular the "rocket problem" was considered, imposing frozen equilibrium, infinite combustion chamber ($M_c = 0$), initial injecting temperatures of the propellant equal to the storage temperatures. The chamber pressure was set as $p_c = 50$ bar and the mixture ratio as $O/F = 2.42$. Latter refinement of this last value will be performed. The output values used from the simulation are represented (vacuum value is considered for the c_T):

c^* [m/s]	c_T [-]	T_c [K]	γ_c [-]	I_{sp} [s]
1851.0	1.935	3709	1.1405	365.22

Table 2: First run on CEAM

From this results, the propellant mass flow rate and the throat area can be calculated:

$$\dot{m}_p = \frac{\mathbb{T}}{c_T c^*} \qquad A_t = \frac{\dot{m}_p c^*}{P_c} \tag{1}$$

From the geometry assumption of Table 1, the nozzle exit area and the combustion chamber geometry can be retrieved:

$$A_e = \varepsilon A_t \tag{2}$$

$$A_c = \varepsilon_{con} A_t \qquad L_c = \frac{L^*}{\varepsilon_{con}} \tag{3}$$

Nozzle geometry model will be delved in section 4. The results for the previous calculation are the following:

$\dot{m}_p$ [kg/s]	D_t [cm]	D_e [cm]	D_c [cm]	L_c [cm]
0.279	1.15	19.86	3.63	11.43

Table 3: Preliminary DRY-1 geometry

A check on the compliance of the chamber Mach number is done ($M_c < 0.3$):

$$\frac{1}{\varepsilon_{con}} = M_c \left[\frac{1 + \frac{\gamma_c - 1}{2}}{1 + \frac{\gamma_c - 1}{2} M_c^2} \right]^{\frac{\gamma_c + 1}{2(\gamma_c - 1)}} \xrightarrow{fsolve} \qquad M_c = 0.059 \tag{4}$$

From the geometry of the motor and the allocated space constraints, the total height of the tanks can be calculated. The volume around the thrust chamber (combustion chamber + convergent) can be assessed:

$$V_{tc} = \frac{\pi}{4}\left[L_c D_c^2 + \frac{L_{con}}{3}\left(D_c^2 + D_t^2 + D_c D_t\right)\right] \tag{5}$$

Also, the volume of the cylinder that covers the length of the thrust chamber and with the total diameter of 1 meter (D_{tot}) can be computed. From there, the empty volume around the thrust chamber can be computed as a difference:

$$V_{lost} = V_{tc} - \frac{\pi}{4}\left(L_c + L_{con}\right) D_{tot} \tag{6}$$

This value must be 20% of the total cylinder volume, as cited in subsection 2.1. As the computed value was lower, additional volume had to be removed from the tanks in order to meet the requirement. The height dedicated to the tanks is calculated as follow:

$$H_{tk} = H - \left[L_c + L_{con} + \frac{4}{\pi D_{tot}^2}\left(0.2 V_{tot} - V_{lost}\right)\right] \tag{7}$$

The total volume allocated to the tanks is hence fully defined. In order to calculate the masses of pressurizer and propellants, some assumption have to be made:

- adiabatic expansion of the pressurizing gas;
- blow-down ratios can be tuned;
- mean value of the oxidizer to fuel ratio.

A system of equations can be set up:

$$\begin{cases} \dfrac{m_{ox}}{m_{fu}} = \overline{O/F} \\ m_{ox} = \rho_{ox} V_{ox} \\ m_{fu} = \rho_{fu} V_{fu} \\ V_{ox} = V_{pr,f}^{ox} - V_{pr,i}^{ox} \\ V_{fu} = V_{pr,f}^{fu} - V_{pr,i}^{fu} \\ V_{pr,f}^{ox} = B_{ox}^{\frac{1}{\gamma_{pr,ox}}} V_{pr,i}^{ox} \\ V_{pr,f}^{fu} = B_{fu}^{\frac{1}{\gamma_{pr,fu}}} V_{pr,i}^{fu} \end{cases} \tag{8}$$

In order to solve System 8, the pressurizer and the initial temperature of the propellants have to be set. Different pressurizing gas are available, mainly nitrogen or helium are the most common choices. The main differences for the two are the storage temperature, the molar mass and the specific heat ratio. The latter parameter influences the adiabatic discharge, higher values implies faster pressure discharge. The molar mass affects the amount of gas to be embarked at a given pressure. The storage temperature is a matter of compatibility with the propellant. Nitrogen gas was chosen to pressurize RP-1 since no cryogenic conditions were present also it guarantees lower discharge, with the downside of increasing the mass of the system. On the other side, LOX required a cryogenic compatibility that can be ensured by helium. Even though an efficient insulating bladder is employed, the design choice was dictated by a more conservative approach. The employment of nitrogen also with LOX was discarded since storage temperature and pressure are not compatible with its properties[6].

$T_{pr,fu}$ [K]	$T_{pr,ox}$ [K]	γ_{N_2} [-]	γ_{He} [-]
300	90	1.40	1.67

Table 4: Initial values for pressurizer gases and specific heat ratio values

$\overline{O/F}$ [-]	$B_{pr,ox}$ [-]	$B_{pr,fu}$ [-]	V_{tot} [m^3]
2.42	2.5	2.5	1.27

Table 5: Assumed or calculated values as first iteration

HO INSERITO I DATI, DOBBIAMO COMMENTARLI
The masses and volumes of oxidizer, fuel and pressurizing gases are computed.

m_{fu} [kg]	m_{ox} [kg]	$V^{fu}_{pr,i}$ [m^3]	$V^{ox}_{pr,i}$ [m^3]	$V_{fu,i}$ [m^3]	$V_{ox,i}$ [m^3]
165.34	400.13	0.2217	0.4789	0.2049	0.3510

Table 6: Propellant and pressurizer quantities as first iteration

HO INSERITO I VALORI TROVATI DALLA PRIMA ITERAZIONE
Finally, the feeding lines can be modelled. Considering figure **REFERENCE** , the length of the pipes can be retrieved as a difference:

$$L_{fd,fu} = H - L_c - H_{tk,fu} \tag{9}$$

$$L_{fd,ox} = H - L_c - H_{tk} \tag{10}$$

To completely determine the DRY-1 geometry, the injection plate must be modelled. The pressure drop across the injector Δp_{inj} have to be assumed as a percentage of the initial chamber pressure. Acceptable range of this fraction goes from 5% to 30%. A value of 20% is chosen for both oxidizer and fuel lines. The fuel and oxidizer injector area can be computed assuming reasonable values for the discharge coefficient $C_{d,inj}$. A reasonable assumption has been made according to the superficial roughness quality of AM.

$$\dot{m}_{fu} = \frac{1}{1+O/F}\dot{m}_p \qquad \dot{m}_{ox} = \frac{O/F}{1+O/F}\dot{m}_p \tag{11}$$

$$A_{inj,tot} = \frac{\dot{m}_p}{C_{d,inj}\sqrt{2\Delta p_{inj}\rho_p}} \tag{12}$$

$$K_p = 1 + f\frac{L_{p,fd}}{D_{p,fd}}\left(\frac{A_{p,fd}}{A_{p,inj,tot}C_{d,inj}}\right)^2 \tag{13}$$

PERDITE DI CARICO GENERALIZZATE

2.3 System dynamics

From the nominal sizing of the engine, it is necessary to simulate the real dynamics of the system in order to:

- retrieve the performance of the designed system in time;
- check the compliance of the system with the constraints;
- test other designs through iteration to select the best one based on the simulated data of interest.

For this reasons, a numerical method was implemented. An high level explanation for the functioning of the algorithm can be appreciated in Figure 2.

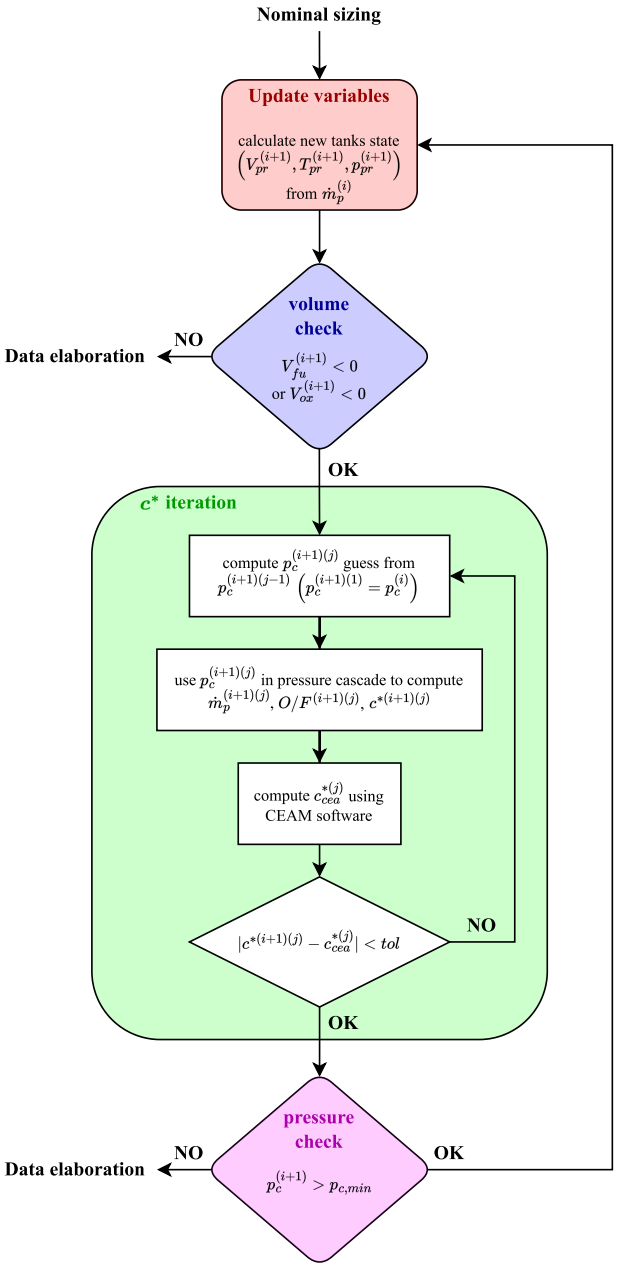

Figure 2: Flowchart of dynamics of the model

The first step of the time cycle is to update the state of the two tanks based on the previous iteration. Assuming a constant propellants flow rate during the time step Δt, the volume of the remaining liquid is decreased by a quantity $\Delta V^{(i+1)}$. Accordingly, the volume of the pressurizer will increase by the same amount.

$$\Delta V^{(i+1)} = \frac{\dot{m}_p^{(i)} \Delta t}{\rho_p} \tag{14}$$

$$V_p^{(i+1)} = V_p^{(i)} - \Delta V^{(i+1)} \tag{15}$$

$$V_{pr}^{(i+1)} = V_{pr}^{(i)} + \Delta V^{(i+1)} \tag{16}$$

From the change of volume, the new pressure and temperature of the pressurizer gas are computed assuming

an adiabatic expansion in the tank:

$$p_{pr}^{(i+1)} = p_{pr}^{(i)} \left(\frac{V_{pr}^{(i)}}{V_{pr}^{(i+1)}} \right)^{\gamma_{pr}} \tag{17}$$

$$T_{pr}^{(i+1)} = T_{pr}^{(i)} \left(\frac{V_{pr}^{(i)}}{V_{pr}^{(i+1)}} \right)^{\gamma_{pr}-1} \tag{18}$$

A check must be performed on the remaining volume of propellants in the tanks at current iteration: if the volume of fuel is negative it means that the combustion is over so the simulation stops (the same for oxidizer). If there is some more propellant to use, the iteration goes on with the calculation of the new chamber pressure. This step is complex because it introduces another cycle of iterations inside each time step. The mass flow rate of the propellants depends on the pressure cascade in the feeding lines, hence on the chamber pressure. These two variables are bounded and both unknown, but there's only one configuration that can match the boundary condition imposed by the critical condition in the throat, so the problem is well-posed.
From literature, the c^* of the chamber has the following expression:

$$c^* = \frac{p_c A_t}{\dot{m}_{fu} + \dot{m}_{ox}} \tag{19}$$

It correlates the chamber pressure with the propellants flow rate in the throat. Moreover, it only depends on the thermodynamics of the combustion process in the chamber, which changes over time due to the architecture of blow-down system. By imposing the critical conditions in the throat, it can be rewritten as:

$$c^* = \sqrt{\frac{\mathcal{R}}{\mathbb{M}} \frac{T_c}{\gamma} \left(\frac{\gamma+1}{2} \right)^{\frac{\gamma+1}{\gamma-1}}} \tag{20}$$

The system is coherent only if the two expressions give the same result. A system of equations could be created and numerically solved to match both the pressure cascade and c^*.
A reasonable initial guess for chamber pressure $p_c^{(i+1)(1)}$ is taken as the pressure at previous time step $p_c^{(i)}$. The next steps $p_c^{(i+1)(j)}$ will converge progressively towards the real current pressure $p_c^{(i+1)}$ (for increasing j).
From $p_c^{(i+1)(j)}$ the $c^{*(i+1)(j)}$ is computed from the pressure cascade as described in Equation 19:

$$u_{fd,p}^{(i+1)(j)} = \sqrt{\frac{2\left(p_{pr}^{(i+1)} - p_c^{(i+1)(j)}\right)}{\rho_p K_p}} \tag{21}$$

$$m_p^{(i+1)(j)} = \rho_p A_{fd,p} u_{fd,p}^{(i+1)(j)} \tag{22}$$

$$O/F^{(i+1)(j)} = \frac{m_{ox}^{(i+1)(j)}}{m_{fu}^{(i+1)(j)}} \tag{23}$$

$$c^{*(i+1)(j)} = \frac{A_t p_c^{(i+1)(j)}}{\dot{m}_{fu}^{(i+1)(j)} + \dot{m}_{ox}^{(i+1)(j)}} \tag{24}$$

Equation 20 is solved directly using CEAM software, which takes as input $p_c^{(i+1)(j)}$ and $O/F^{(i+1)(j)}$ to return $c_{cea}^{*(j)}$.
The two computed c^* are then compared: if their difference satisfies a certain tolerance, then the cycle stops and returns the new values for the current time step. Else, the inner cycle continues the refinement by guessing a new $p_c^{(i+1)(j+1)}$ from $p_c^{(i+1)(j)}$.
Finally, a check on the new combustion pressure $p_c^{(i+1)}$ is performed in order to stay above the minimum design pressure $p_{c,min}$, as mentioned in subsection 2.1. Similarly to the previous check, if the pressure drops below the limit the simulation stops and returns the results, else it continues with the next time step.

The same general algorithm is used to refine the initial assumptions of O/F and B, which influence the nominal design of the whole engine (as described in subsection 2.2). In this case, the initial c^* value from design is assumed constant to reduce the computational burden, since the algorithm is applied over a wide range of combinations of O/F and B. This assumption is reasonable because the O/F (and as consequence the thermodynamics of the combustion) hardly varies during the whole burn, as can be noticed in Figure 5.

3 Results analysis

DRY-1 final design, as mentioned in subsection 2.2, maximizes the total specific impulse deliverable while respecting all the constraints and the assumptions of the model discussed in subsection 2.1. It is obtained through the iteration of the code presented in subsection 2.3, varying all the nominal design parameters (geometry included) as function of the selected DOFs: B and O/F. In this part all the losses in the nozzle were neglected. They will be discussed off-design in section 4 to evaluate the behavior of the engine in more realistic conditions. Also the possible non-nominalities in the realization of the injection plate and the possible strategies to cool down the system are separately treated, respectively in section 5 and section 6.
In the present section the obtained design will be presented and analyzed through the most relevant parameters, plotted vs time of burn to see the evolution of the system.

$\overline{O/F}$ [-]	$B_{pr,ox}$ [-]	$B_{pr,fu}$ [-]
2.35	2.78	2.78

Table 7: DRY-1 optimal design values

c^* [m/s]	c_T [-]	T_c [K]	I_{sp} [s]	I_{tot} [Ns]
1856.3	1.932	3692	355.79	$2.173 \cdot 10^6$

Table 8: Performance parameters for DRY-1

$\dot{m}_{fu}$ [kg/s]	$\dot{m}_{ox}$ [kg/s]
$8.322 \cdot 10^{-2}$	$1.956 \cdot 10^{-1}$

Table 9: Mass flow rates for DRY-1

D_t [cm]	D_e [cm]	D_c [cm]	L_c [cm]
1.15	19.88	3.63	11.43

Table 10: Geometry for DRY-1

m_{fu} [kg]	m_{ox} [kg]	$V^{fu}_{pr,i}$ [m^3]	$V^{ox}_{pr,i}$ [m^3]	$V_{fu,i}$ [m^3]	$V_{ox,i}$ [m^3]
182.45	428.67	0.2102	0.4441	0.2261	0.3761

Table 11: Tanks sizing for DRY-1

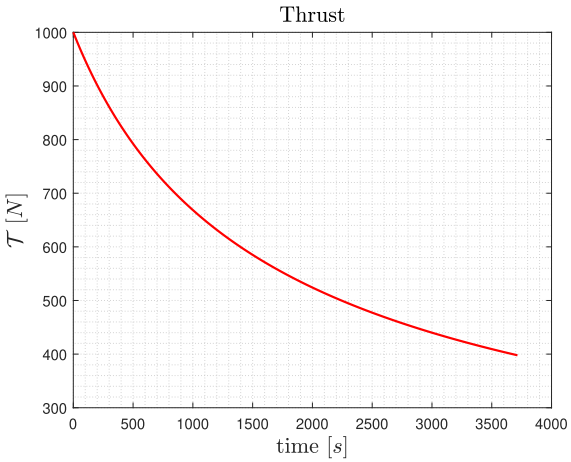

Figure 3: Thrust

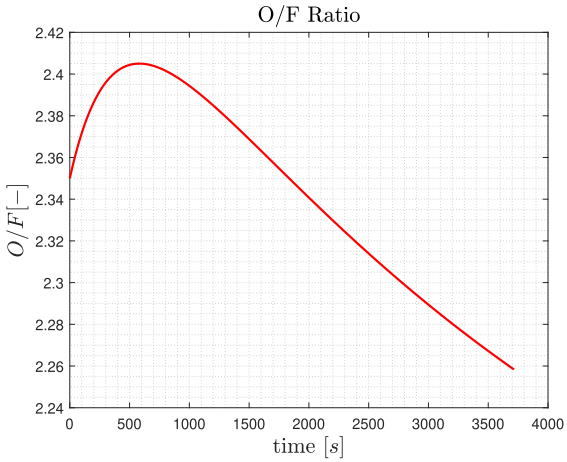

Figure 4: O/F ratio

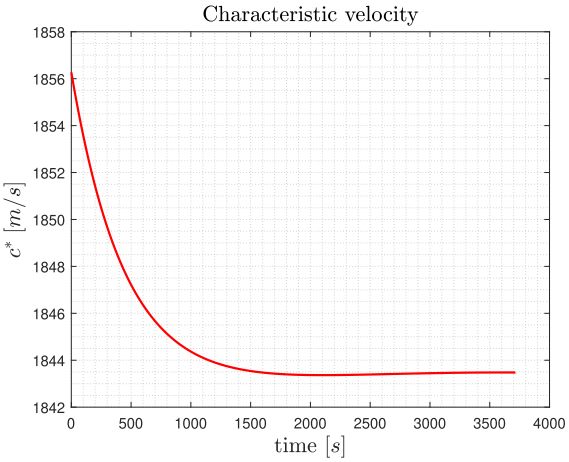

Figure 5: Characteristic velocity

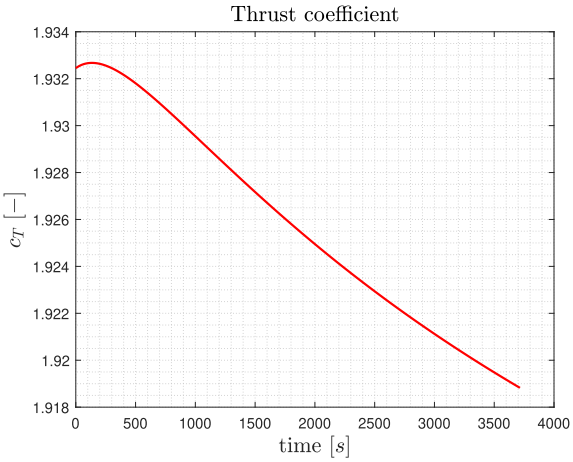

Figure 6: Thrust coefficient

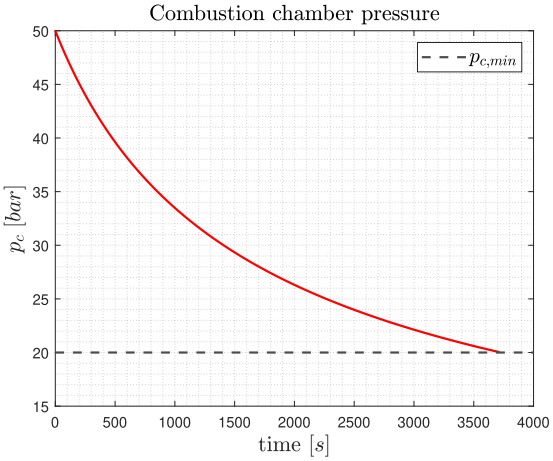

Figure 7: Combustion chamber pressure

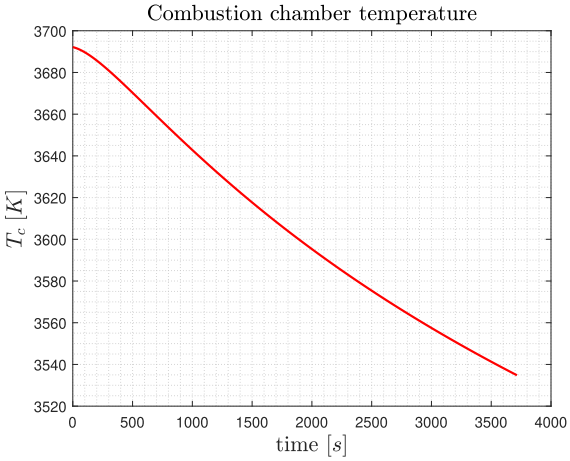

Figure 8: Combustion chamber temperature

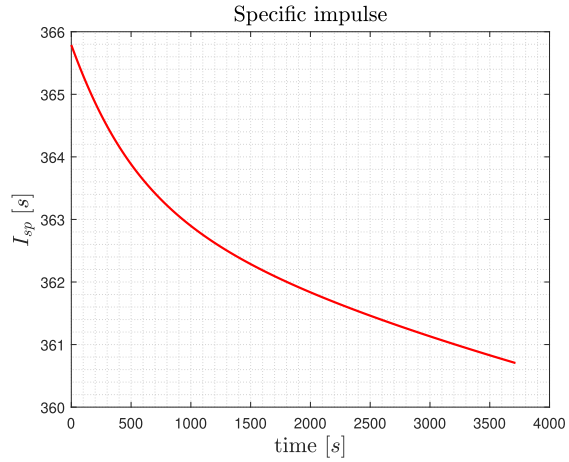

Figure 9: Specific impulse

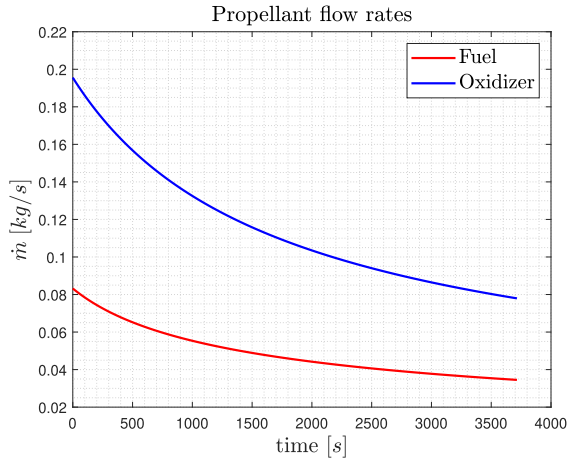

Figure 10: Propellant flow rates

Some general consideration from the graphs can be made.

- The pressure and the temperature in the combustion chamber decreases in time as a consequence of the discharge of the tanks. Thrust and specific impulse diminish as well since they depend on these values.
- Since the combustion is less effective, the characteristic velocity, which depends uniquely on the thermodynamics of the chamber, lower its initial value. Despite this, the global variation is negligible, so it

can be assumed constant to reduce the calculation burden on the dynamics (as already mentioned in subsection 2.3).

- O/F ratio barely changes during the time of burn. It has a peculiar evolution with respect to the other monotonic developments: it firstly increases and then decreases. This is mainly imputable to the difference in pressurizers chosen for the two tanks, which have different performances: helium discharges the oxidizer more rapidly with respect to nitrogen, which has a less steep and more constant discharge in time (Figure 10).
- A similar development can be found in the thrust coefficient: this is due to the fact that in vacuum its value depends only by the geometry of the nozzle (which is fixed) and by the specific heat ratio of the exhaust gases. The latter depends on the chemistry of the mixture, but it does not strictly follow the O/F ratio.

4 Nozzle losses

5 Additive manufacturing influences

6 Cooling analysis

Bibliography

[1] Robert-Jan Koopmans et Al. “Propellant Tank Pressurisation with Helium Filled Hollow Glass Microspheres”. In: (2015).

[2] H. C. Hearn. “Design and Development of a Large Bipropellant Slowdown Propulsion System”. In: (1995).

[3] G.P.Sutton. “Rocket Propulsion Elements”. In: (2017).

[4] Ariane Group. *Chemical bipropellant thruster family*. Site: https://www.space-propulsion.com/. 2021.

[5] Huzel and Huang. “Modern Engineering for design of Liquid-Propellant Rocket Engines”. In: (1992).

[6] *NIST Chemistry WebBook*. URL: https://webbook.nist.gov/cgi/fluid.cgi?T=85&PLow=4&PHigh=5.5&PInc=0.1&Digits=5&ID=C7727379&Action=Load&Type=IsoTherm&TUnit=K&PUnit=bar&DUnit=mol%2Fl&HUnit=kJ%2Fkg&WUnit=m%2Fs&VisUnit=Pa*s&STUnit=N%2Fm&RefState=DEF. (accessed: 14.04.2024).